

RESEARCH ARTICLE

View Article Online
View Journal | View IssueCite this: *Org. Chem. Front.*, 2015, **2**, 783

Mechanistic studies on C–C reductive coupling of five-coordinate Rh(III) complexes†

Shanshan Chen,^{a,c} Yan Su,^b Keli Han^b and Xingwei Li^{*a,b}

A series of five-coordinate Rh(III) vinyl complexes [Rh(N[^]C)(PAR₃)₂CH=CHR]PF₆ have been isolated as an intermediate in the coupling of a Rh(III) hydride with terminal alkynes. These Rh(III) vinyl complexes underwent aryl–vinyl reductive coupling to afford the Rh(I) chelating complex [Rh(N[^]C–CH=CHR)–(PAR₃)₂]PF₆ in high yields. Kinetic studies on the C–C reductive elimination revealed that the reaction kinetics is first order for a Rh(III)(4-trifluoromethyl)styryl complex with activation parameters of $\Delta H^\ddagger = 20.9$ kcal mol⁻¹ and $\Delta S^\ddagger = -6.1$ eu. The electronic effects of the styryl group and the phosphine ligands on the rate of C–C reductive elimination were studied, and the rate constant decreases for a more electron-poor styryl group but increases for a less donating phosphine. The inhibitive effect of the added phosphine indicates that the dissociation of phosphine to afford a four-coordinate intermediate is involved, which was further supported by DFT calculations. Although intermediacy of a 4-coordinate species has been suggested, the active intermediate that directly undergoes C–C coupling was pinpointed to a five-coordinate *cis* phosphine complex on the basis of DFT studies. Significant accelerating effects were observed for oxygen donor solvents (THF-*d*₈ and acetone-*d*₆), possibly *via* efficient stabilization of the four-coordinate intermediate. However coordination of CO forms an inert six-coordinate Rh(III) complex. Thus an overall detailed mechanism of alkyne insertion and subsequent aryl–vinyl reductive elimination from the Rh(III) center has been proposed based on the experimental and theoretical data.

Received 9th February 2015,
Accepted 28th April 2015

DOI: 10.1039/c5qo00049a

rsc.li/frontiers-organic

Introduction

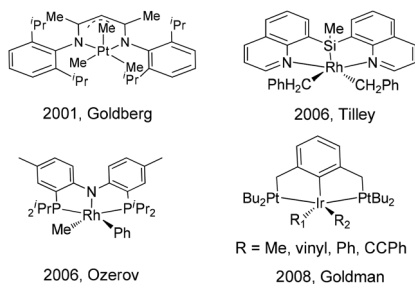
Transition-metal catalyzed C–C bond formation reactions *via* direct C–H bond activation have been increasingly developed in organic synthesis during the past several decades.^{1–14} Among these reactions, the reductive elimination of a C–C bond is one of the most important elementary steps because in many catalytic systems this is the product-forming step. Experimental and computational studies of C(sp³)–C(sp³), C(sp³)–C(sp²), C(sp²)–C(sp²) reductive elimination from palladium and platinum complexes have been extensively explored.^{15–24} However, the mechanism and controlling factors in C–C reductive elimination from other transition-metal complexes (Rh, Ir, Ru, Os, Co) are relatively less studied.^{25–35}

According to the reported mechanistic studies, C–C reductive elimination from d⁶ transition-metal complexes often proceeds *via* a five-coordinate intermediate,^{36–39} which is generated by ligand dissociation. In many cases, the five-coordinate intermediate is relatively unstable and is hardly isolable, which defies subsequent detailed mechanistic studies. As far as we know, only a few stoichiometric C–C coupling systems with authenticated five-coordinate intermediates have been documented. For example, a series of five-coordinate Pt(IV) alkyl intermediates bearing nitrogen pincers have been isolated and characterized by Goldberg,⁴⁰ Tilley,⁴¹ Wang,⁴² and Song.⁴³ Goldman reported a series of five-coordinate iridium(III) pincer complexes (PCP)Ir(R)(R') (R = alkyl, vinyl, aryl, alkynyl), which were synthesized from the corresponding RX and R'Li reactants. However, these intermediates were not stable for isolation, and they were only characterized by ¹H and ³¹P NMR spectroscopy and by X-ray crystallography in their six-coordinate derivatives.⁴⁴ Five-coordinate (PNP)Rh(R)(R') pincer intermediates that can reductively eliminate have been reported by Ozerov, but their structures were only proposed on the basis of spectroscopic characterization (Scheme 1).⁴⁵

On the other hand, very recently, rhodium(III)-catalyzed C–H activation/C–C coupling reactions have been increasingly explored and a vast majority of efficient synthetic methods have been developed.^{8,11,13} These methods also offered impor-

^aDivision of Chemistry and Biological Chemistry, School of Physical and Mathematical Sciences, Nanyang Technological University, Singapore 637371^bDalian Institute of Chemical Physics, Chinese Academy of Sciences, Dalian 116023, China. E-mail: xwli@dicp.ac.cn^cDepartment of Applied Chemistry, School of Sciences, Anhui Agricultural University, Hefei 230036, China

† Electronic supplementary information (ESI) available: Detailed information on the syntheses, characterization data of all rhodium complexes, X-Ray crystal data (2ab, 3aa and 3ak), and the kinetic results. CCDC 1008419–1008421. For ESI and crystallographic data in CIF or other electronic format see DOI: 10.1039/c5qo00049a



Scheme 1 Reported five-coordinate intermediates in stoichiometric coupling.

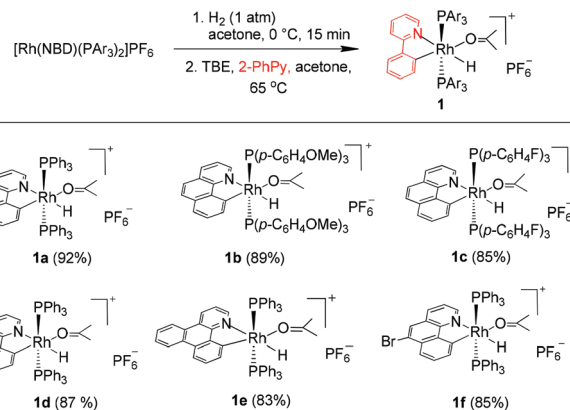
tant synthetic complements to palladium- and ruthenium-catalyzed C–H activation/C–C coupling reactions. The C–C reductive elimination of a Rh(III) complex is particularly important because it is proposed as a key product-forming step in many catalytic systems with a Rh(III)/Rh(I) cycle. Despite the significance, only a few reports detailed the stoichiometric C–C reductive elimination of Rh(III) complexes,^{27,35,41b,45} which stands in sharp contrast to the majority of reports on stoichiometric C–C and C–N coupling of palladium complexes. Inspired by the above reports, we aim to synthesize a range of rhodium(III) complexes to delve into the mechanism of subsequent C–C reductive coupling using a combination of experimental and theoretical methods.

Results and discussion

In 2003, Crabtree and coworkers reported the double insertion of a terminal alkyne into a cyclometalated iridium(III) hydride to afford a butadienyl complex, with the cyclometalated ligand being a spectator.^{27a} In contrast to iridium, rhodium generally forms a weaker M–C bond. Therefore, the interactions of Rh(III) hydrides with alkynes may follow a different reaction pattern. Thus the cyclometalated ligand might act as a participating group in subsequent C–C coupling.

Synthesis of [Rh(N[^]C)(PAR₃)₂(CH=CHR)]PF₆ intermediate **2**

We reasoned that the insertion of a terminal alkyne into a stable rhodium aryl hydride may afford an isolable alkenyl complex that can be a suitable candidate for subsequent C(aryl)–C(alkenyl) coupling studies. This is based on the rationale that a Rh–C(aryl) bond is usually kinetically more labile than the iridium counterpart. To achieve this goal, a series of cyclometalated rhodium(III) hydride complexes **1** have been prepared *via* cyclometalation according to our previously reported procedure in the presence of *tert*-butylethylene (TBE) (Scheme 2).⁴⁶ All these hydride complexes were fully characterized and, in particular, the hydride signal resonates as a doublet of triplets in a narrow range of δ –12.13 to –12.49 in the ¹H NMR spectroscopy and the Rh–C resonates as a doublet of triplets (δ 153.08 to 163.83) in ¹³C NMR spectroscopy (acetone-*d*₆).



Scheme 2 Synthesis of rhodium hydrides.

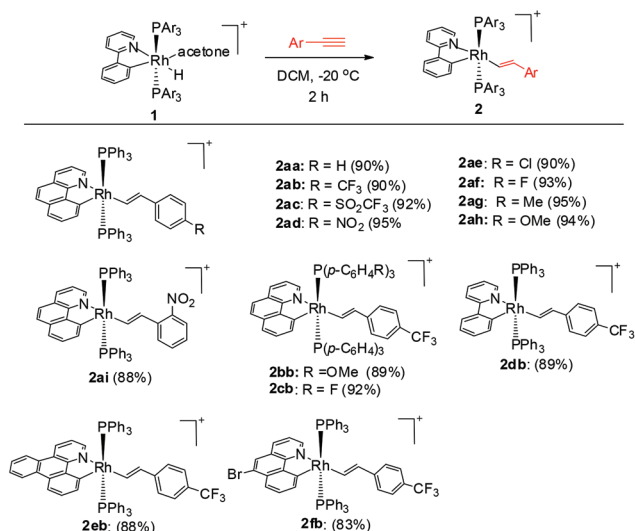
Isolation of five-coordinate Rh(III) alkenyl complexes

To our delight, stirring a mixture of hydride **1a** and an excess of (4-trifluoromethyl)phenylacetylene in DCM at –20 °C led to a red solution with the clean formation of a Rh(III) *trans*-styryl complex **2ab**, although the reaction at rt afforded a Rh(I) C–C coupled product (*vide infra*). Rapid removal of the solvent followed by washing with diethyl ether afforded **2ab** in analytical purity in 90% yield. Complex **2ab** was fully characterized at –20 °C. On the basis of ¹H NMR spectroscopy, only one equiv. of alkyne was incorporated and a characteristic doublet of triplets signal at δ 8.36 (dt, ³J_{HH} = 17.0 Hz, ³J_{PH} = 5.5 Hz) was observed and was assigned to the β proton of the *trans*-styryl unit (Rh–CH = CH(C₆H₄)CF₃). The other olefinic CH was detected at δ 5.13 (d, ³J_{HH} = 17.0 Hz). Furthermore, no ligated acetone could be detected by ¹H NMR spectroscopy, indicating that complex **2a** might be five-coordinate. In the ¹³C NMR spectrum, two Rh–C signals were detected each as a triplet of doublets at δ 145.08 (dt, ²J_{RhC} = 42.9 Hz, ³J_{PC} = 9.2 Hz, Rh-aryl) and δ 153.65 (dt, ²J_{RhC} = 32.2 Hz, ³J_{PC} = 10.7 Hz, Rh-styryl). In the ³¹P NMR spectrum, a doublet signal (δ 23.4, ¹J_{RhP} = 112.1 Hz) was observed for the two equivalent phosphorus atoms, indicative of their *trans* orientation.

By following this procedure, a series of terminal alkynes bearing various electron-donating and -withdrawing substituents underwent smooth insertion into the Rh–H bond to afford the corresponding Rh(III) alkenyl complexes in high yields (Scheme 3). These results stand in contrast to the facile double insertion of alkyne into the iridium congener of rhodium hydrides **1**, where the insertion of the 2nd equiv. of alkyne into the Ir–vinyl bond readily proceeded so that no iridium(III) vinyl intermediate could be isolated in a less coordinating solvent such as DCM.^{27a}

Crystal structure

Single crystals of **2ab** suitable for X-ray crystallographic studies were obtained by slow diffusion of diethyl ether to a dichloromethane solution at –20 °C. X-ray crystallographic studies unambiguously confirmed the identity of **2ab** (Fig. 1). As



Scheme 3 Synthesis of five-coordinate vinyl complexes.

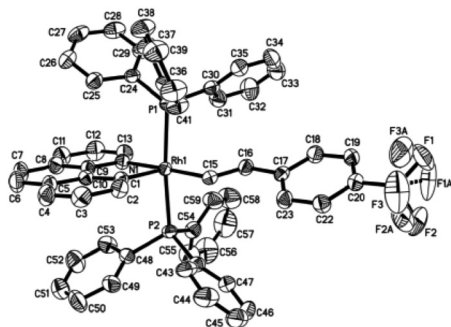


Fig. 1 Molecular structure (ORTEP) of the cation of **2ab** with thermal ellipsoids shown at the 50% probability level. Selected bond lengths (Å) and angles (°): Rh1–C1, 1.987(3); Rh1–C15, 2.019(3); Rh1–N1, 2.145(3); Rh1–P2, 2.3448(10); Rh1–P1, 2.3503(9); C15–C16, 1.337(5); C1–Rh1–C15, 100.04(14); C1–Rh1–N1, 81.82(13); C15–Rh1–N1, 177.27(13); C1–Rh1–P2, 91.35(11); C15–Rh1–P2, 87.56(10); N1–Rh1–P2, 90.41(9); C1–Rh1–P1, 93.90(11); C15–Rh1–P1, 89.10(10); N1–Rh1–P1, 92.77(9); P2–Rh1–P1, 174.20(3).

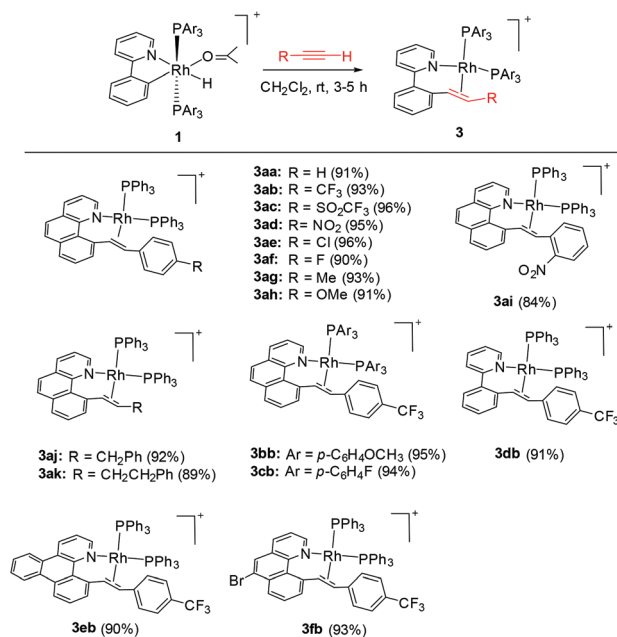
depicted in Fig. 1, the two PPh₃ ligands are mutually *trans* and the coordination sphere involves five regular bonds, while the sixth coordination site is unoccupied and is *trans* to the high *trans*-effect aryl ligand. No secondary interaction between the rhodium center and the styryl group could be detected. Therefore this Rh(III) styryl complex represents a rare example of a five-coordinate d⁶ complex generated from the insertion of an alkyne into a metal hydride.

C–C reductive elimination of the vinyl complexes

It has been well studied that metal complexes with coordinative unsaturation tend to undergo facile reductive elimination.^{36–39} Thus, we reasoned that our coordinatively unsaturated and fluxional complexes **2** might be labile toward

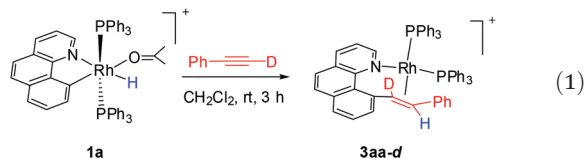
reductive coupling, and consequently they may be a suitable subject for stoichiometric studies. Indeed, dissolution of the five-coordinate vinyl complex **2ab** in CD₂Cl₂ at room temperature led to clean and quantitative formation of the C–C coupled product **3ab** within hours. Alternatively, this product could be isolated in a similar yield directly from the room temperature reaction of rhodium hydride **1a** and (4-trifluoromethyl)phenylacetylene. The reductively coupled product was fully characterized by NMR spectroscopy and X-ray crystallography. In the ¹H NMR spectrum of **3ab** (CD₂Cl₂), two doublets resonate at δ 6.48 ppm and δ 5.50 ppm and were assigned to the α and the β protons in the styryl unit, respectively, on the basis of HMBC and HMQC spectroscopy. The observed coupling constant (13.8 Hz) between these two protons is slightly less than 16 Hz as a result of the change in the hybridization to a more sp³ character, suggestive of a metal-bound olefin group. In the ¹³C NMR spectrum (CD₂Cl₂), the two olefinic carbon signals were detected at δ 78.6 (dd, ²J_{RhC} = 19.9 Hz, ³J_{PC} = 6.2 Hz) and δ 85.0 (d, ²J_{RhC} = 12.1 Hz). The *ipso* carbons of the phenyl groups in PPh₃ appear as a doublet at δ 130.6 (¹J_{PC} = 45.8 Hz) and 130.9 (¹J_{PC} = 41.1 Hz) with no virtual coupling, indicative of the *cis* orientation of the PPh₃ ligands. In line with the ¹³C NMR data, the ³¹P NMR spectrum gave two mutually coupled signals at δ 30.95 (dd, ¹J_{RhP} = 169.4 Hz, ²J_{PP} = 44.5 Hz) and 36.21 (dd, ¹J_{RhP} = 155.6 Hz, ²J_{PP} = 44.0 Hz), the latter signal being assigned to the PPh₃ *trans* to the olefin ligand, where the smaller *J*_{Rh–P} is caused by the high *trans*, labilizing effect of the olefin.

By following this generic procedure, C–C reductively coupled products were conveniently prepared in a broad scope from the room temperature reaction between the Rh(III) hydride complex and a terminal alkyne (Scheme 4). Since this



Scheme 4 Synthesis of Rh(I) olefin complexes via C–C coupling.

process involved the insertion of alkyne into a rhodium(III) hydride, deuterium labeling studies have been performed using **1a** and phenylacetylene-*d* (eqn (1)). ¹H NMR analysis of the isolated Rh(I) olefin complex revealed that the deuterium was located exclusively at the carbon adjacent to the benzo[*h*]-quinoline unit. This suggests no cleavage of the alkynyl C–H bond during the insertion of the alkyne, hence ruling out the intermediacy of a vinylidene species.



Crystal structure of Rh(I) products

Single crystals of **3aa** and **3ak** suitable for X-ray crystallographic studies were obtained by the slow diffusion of diethyl ether to their dichloromethane solutions at room temperature (Fig. 2 and 3). As shown in Fig. 2, **3aa** is best described as a square planar complex and the coordination sphere includes a chelating pyridine-olefine ligand and two *cis* PPh₃ ligands. The benzo[*h*]quinoline ring is slightly twisted to accommodate this chelation mode in a rather sterically congested setting. Detailed crystallographic data on complexes **3aa** and **3ak** are provided in the ESI.†

Although the five-coordinate vinyl complexes readily coupled at room temperature, bubbling CO through a solution of **2ab** led to the formation of a six-coordinate carbonyl complex **4** which was isolated in quantitative yield (eqn (2)). The CO occupies the sixth site to give a stable Rh(III) complex so that no C–C reductive elimination was observed. This obser-

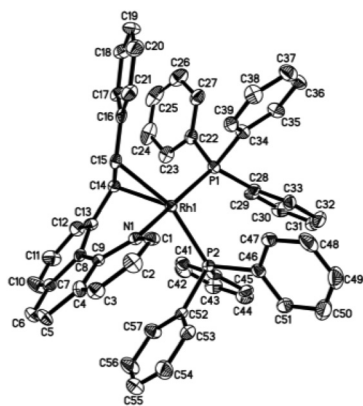


Fig. 2 Molecular structure (ORTEP) of the cation of **3aa** with thermal ellipsoids shown at 50% probability. Selected bond lengths (Å) and angles (°): Rh1–N1, 2.093(4); Rh1–C14, 2.158(5); Rh1–C15, 2.300(5); Rh1–P1, 2.3042(12); Rh1–P2, 2.3192(13); C14–C15, 1.427(7); N1–Rh1–C14, 87.63(17); N1–Rh1–C15, 77.94(16); C14–Rh1–C15, 37.16(18); N1–Rh1–P1, 168.90(11); C14–Rh1–P1, 99.18(13); C15–Rh1–P1, 102.22(12); N1–Rh1–P2, 87.51(11); C14–Rh1–P2, 131.52(13); C15–Rh1–P2, 161.16(13); P1–Rh1–P2, 94.37(5).

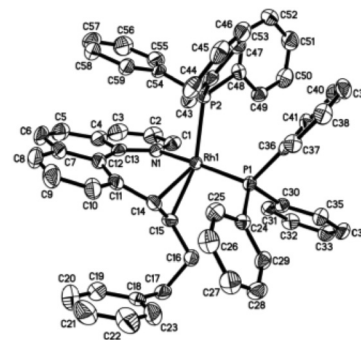
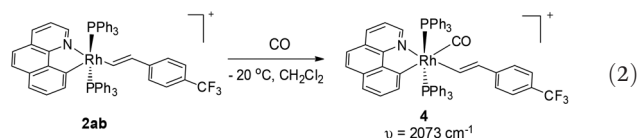


Fig. 3 Molecular structure (ORTEP) of the cation of **3ak** with thermal ellipsoids shown at 50% probability. Selected bond lengths (Å) and angles (°): Rh1–N1, 2.098(3); Rh1–C14, 2.127(5); Rh1–C15, 2.224(4); Rh1–P1, 2.2925(11); Rh1–P2, 2.3420(11); C14–C15, 1.405(7); N1–Rh1–C14, 87.42(17); N1–Rh1–C15, 79.50(15); C14–Rh1–C15, 37.59(17); N1–Rh1–P1, 167.70(11); C14–Rh1–P1, 97.29(14); C15–Rh1–P1, 97.30(12); N1–Rh1–P2, 88.21(10); C14–Rh1–P2, 130.15(13); C15–Rh1–P2, 162.41(13); P1–Rh1–P2, 97.264.

vation further indicates that C–C reductive elimination tends to occur preferentially for coordinatively unsaturated species.



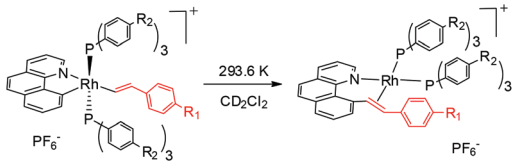
Kinetic studies

Kinetic parameters for the conversion of **2ab** to **3ab** were experimentally assessed by monitoring the decay of **2ab** by ¹⁹F NMR spectroscopy in CD₂Cl₂ to reveal $k = 2.28(1) \times 10^{-3} \text{ min}^{-1}$ at 287.7 K. The reaction was found to obey first-order kinetics. The rate constants measured at different temperatures are displayed in Table 1. Temperature dependence studies of the **2ab** to **3ab** conversion allowed for the extraction of the activation parameters $\Delta H^\ddagger = 20.9(3) \text{ kcal mol}^{-1}$ and $\Delta S^\ddagger = -6.1(3) \text{ cal (mol K)}^{-1}$ from the Eyring plot. This negative value of ΔS^\ddagger suggests that the transition state is slightly more ordered than the ground state. However, the ΔS^\ddagger value is not significant enough to warrant conclusive discussion of the mechanism.

To gain further insight into the mechanism of this reductive elimination, the electronic effect of the reactive styryl group has been perturbed. It was found that the introduction of a more electron-donating substituent into the *para* position of the phenyl ring in the styryl group resulted in a more rapid

Table 1 Temperature-dependent kinetics for the decay of **2ab**

Entry	<i>T</i> (K)	<i>k</i> (min ⁻¹)
1	287.7	0.00228(1)
2	293.6	0.00471(7)
3	297.0	0.00704(4)
4	305.3	0.0197(1)

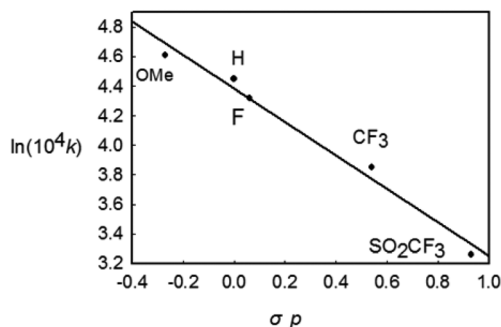
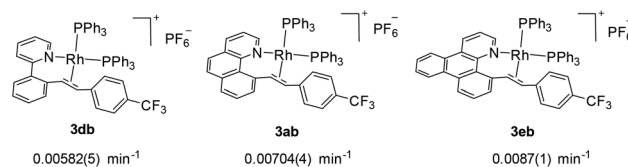
Table 2 Electronic effects of reacting and ancillary ligands (293.6 K)


Entry	R ₁	R ₂	σ_p (R ₁)	k (min ⁻¹)
1	OMe	H	-0.27	0.0101(1)
2	H	H	0	0.0086(1)
3	F	H	0.06	0.0079(1)
4	CF ₃	H	0.65	0.00471(7)
5	SO ₂ CF ₃	H	0.93	0.00255(2)
6	CF ₃	OMe		0.00410(6)
7	CF ₃	F		0.00684(3)

decay (Table 2, entries 1–5), and the most electron-withdrawing substituent $-\text{SO}_2\text{CF}_3$ gave the lowest rate. The linear free energy correlation between the rate constant and the σ_p of the *para* substituent gave a straight line ($R^2 = 0.955$). An alternative plot using the resonance substituent constant σ_p^+ also gave a straight line with $R^2 = 0.954$, indicating that the resonance effects probably have a dominant influence on the rate of the coupling reaction (Chart 1). On the other hand, the reaction occurred faster for more electron-poor ancillary phosphine ligands (entries 1, 6, and 7). These observations are typical and are consistent with those in most kinetic studies on the (concerted) reductive elimination of Pd(II) complexes,²⁰ where these two baseline electronic effects are attributed to the electronic effects of the ground state.

Effects of cyclometalated ligands

We next investigated the effects of the reactive cyclometalated aryl ligand, and the data are given in Scheme 5. It was found that an aryl group with extended conjugation gives a higher rate, although this effect is not significant. This observation seems counterintuitive in terms of the ground state electronic effects because an extended conjugated aryl group tends to facilitate π -back donation to give a stronger Rh–Aryl bond.

**Chart 1** The Hammett plot for the decay of Rh(III) complexes bearing different *p*-substituents in the styryl group.**Scheme 5** Effects of the cyclometalated aryl ligands on the rate of C–C reductive coupling (297.0 K, CD₂Cl₂).**Table 3** Solvent effects on the kinetics of decay of **2ab** to **3ab** at 281 K

Entry	Solvent	Dielectric constant	k (min ⁻¹)
1	CD ₂ Cl ₂	9.1	0.000958 (extrapolated)
2	THF- <i>d</i> ₈	7.5	0.0214(2)
3	Acetone- <i>d</i> ₆	21	0.0231(2)

However, this observation may be ascribable to transition state stabilization or stabilization of the ligated olefin product, where a more rigid chelating N[^]C group gives a better stabilized π -olefin complex. Clearly, pre-decoordination of the pyridyl group is unlikely because in this case the 2-phenylpyridyl ligand is most flexible among all the three and the decay of **2db** to **3db** would have been fastest.

The solvent effects

The effect of solvents on the reductive elimination has also been investigated (Table 3). Reactions conducted at 281 K in a weakly coordinating, oxygen-containing solvent such as acetone-*d*₆ and THF-*d*₈ occurred significantly faster than in CD₂Cl₂, but there is no correlation between the dielectric constant of the solvent and the reaction rate. Instead, the donating capacity of the solvent seems to play an important role, possibly by stabilization of a cationic, unsaturated four- or five-coordinate intermediate.

The fact that the reductive coupling occurred at a higher rate in a more coordinating solvent simply suggests that the reaction proceeds either *via* a four coordinate or a five coordinate intermediate such as a five coordinate diphosphine or a PPh₃/solvent complex. Furthermore, the PPh₃/solvent intermediate is quite unlikely when CH₂Cl₂ was used as a solvent. To gain further insight, the effect of added phosphine has been examined.

Effects of added phosphine ligands

To explore whether the reductive elimination occurs *via* a four-coordinate Rh(III) intermediate *via* phosphine dissociation, phosphine concentration-dependent kinetic studies have been performed at 297 K (Table 4). It was found that the decay of **2ab** was slightly inhibited with the introduction of various amounts of PPh₃. On the other hand, ³¹P and ¹⁹F NMR spectroscopy revealed that no new phosphine-containing species was generated and the only detectable species are **2ab** and PPh₃. This indicates that the initial concentration of **2ab** was

Table 4 Phosphine concentration-dependent kinetics for the decay of complex **2ab** (297 K, CD₂Cl₂)

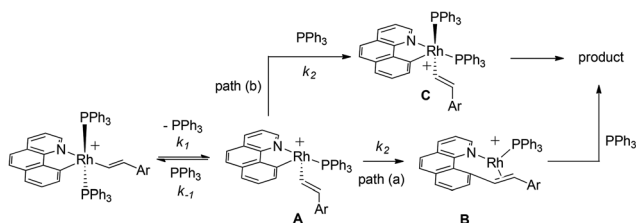
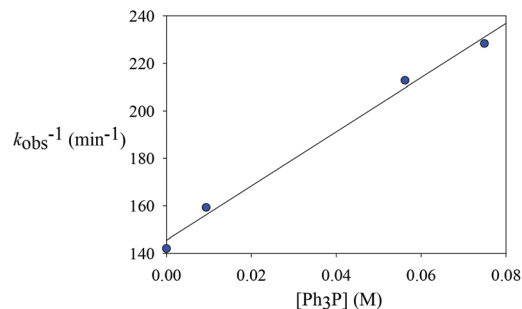
Entry	[PPh ₃] (M)	<i>k</i> _{obs} (M ⁻¹ min ⁻¹)
1	0	0.00704(4)
2	0.00936 (1 equiv.)	0.00628(13)
3	0.0562 (6 equiv.)	0.0047(1)
4	0.0749 (8 equiv.)	0.00438(4)

not affected upon addition of PPh₃ and the starting five-coordinate rhodium species is not a directly reactive species. Instead, reversible phosphine dissociation to afford a reactive four-coordinate monophosphine intermediate was suggested and is kinetically important, and the formation of such a four-coordinate species was inhibited by the introduction of phosphine. Indeed, this proposal of four-coordinate species seems to correlate well with the solvent effect. This reactive four-coordinate species was stabilized by weakly coordinating solvents such as acetone and THF by oxygen binding, leading to a more rapid decay.

Postulated elementary steps for the decay of **2ab** to **3ab** are depicted in Scheme 6. In path (a), phosphine dissociation generates a four-coordinate intermediate, which undergoes reorganization (A) and reductive elimination to afford a three-coordinate olefin intermediate (B). The final product was produced with the rapid recoordination of the PPh₃. Alternatively (path (b)), the four-coordinate intermediate A may be trapped by PPh₃ to give a *cis* phosphine intermediate C, C-C coupling of which furnishes the final product. These two pathways are kinetically undistinguishable by experimental methods if the steps after the formation of the four-coordinate intermediate are not rate-determining.

$$k_{\text{obs}} = \frac{k_1 k_2}{k_{-1} [\text{PPh}_3] + k_2} \quad (3)$$

When the steady state approximation was applied to the four-coordinate intermediate, a rate law given in eqn (3) can be derived, assuming that the recoordination of PPh₃ to give C or C-C coupling to give B is rapid and kinetically unimportant. Indeed, a plot of the reciprocal of *k*_{obs} against [PPh₃] does show a fairly good straight line (Chart 2). Based on this plot, the rate constant of the dissociation of the PPh₃ (*k*₁) was estimated to be 6.9 × 10⁻³ min⁻¹ and a ratio of *k*₋₁/*k*₂ was calculated from the slope to be 7.8.

**Scheme 6** Possible reaction pathways.**Chart 2** The effects of added phosphine.

The DFT method

For the calculation of the free energy associated with the elementary process which involves adduct formation between the Rhodium complex and phosphine and the process which involves dissociation of the phosphine from the Rhodium complex, entropy effects should be taken into consideration.

We evaluate free energy change at 298 K by two ways. In one way, translation, rotation, and vibration movements are taken into consideration to estimate the thermal entropy and free energy, where all substrates are treated as the ideal gas. In the other way, only the vibration movements are considered in the estimation of the thermal energy and free energy, but translation and rotation movements are neglected, because in the solution the translation and rotation movements are highly suppressed. In the former method, entropy significantly decreases upon the formation of adduct from two molecules, as expected. In the latter method, on the other hand, formation of adduct induces a very small entropy change, as will be discussed below. The former method apparently overestimates the entropy effects and the thermal energy of the solution reaction, because translation and rotation movements are highly suppressed in solution. On the other hand, the latter method underestimates the entropy effects and the thermal energy, because translation and rotation movements are not completely suppressed in solution. The true value would be intermediate between the value (ΔG°) obtained by the former method and that (ΔG_v°) by the latter one, and more or less close to the free energy change estimated by the latter method, when the reaction is carried out in solution.

Because this ambiguity remains in the estimation of the entropy and thermal energy, we will discuss each elementary step based on the usual total energy changes with zero-point energy correction (ΔE). Of course, the free energy change does not differ so much from the total energy change in the elementary steps that involve neither the formation of adduct nor the release of product. Also, the free energy change that is evaluated by considering only vibration movements does not differ so much from the total energy change. The significant difference between the free energy change and the total energy change is observed in the elementary process that involves either the formation of adduct or the release of product, when

translation, rotation, and vibration movements are considered in the estimation of free energy.

All the DFT calculations were carried out using the GAUSSIAN 09 series of programs. Density functional theory and B3LYP with a standard 6-31+G(d) basis set (SDD basis set for Rh) were used for geometry optimizations. The solvent effects were considered by single point calculations on the gas-phase stationary points with a SMD continuum solvation model.

DFT studies

Theoretical studies at the DFT level have been performed (Scheme 7). It was found that the initial phosphine dissociation occurs with $\Delta G = 22.1$ kcal mol⁻¹ because this process is unfavorable in both entropy and enthalpy. Int₁ readily isomerizes by Berry pseudorotation to produce a slightly more stable four coordinate Int₂ with a minimal barrier, where the styryl group is oriented to the apical position. DFT studies suggest that path (a) is unlikely because a rather high free energy of 34.9 kcal mol⁻¹ (18.1 kcal mol⁻¹ for this step) was located for the TS_{2a} when Int₂ directly reductively eliminates to give Int_{3a}. In contrast, by following path (b), PPh₃ binding to Int₂ gives Int_{3b} with slight exergonicity. Thus the conversion of the starting complex to Int_{3b} represents a facile stepwise *trans* to *cis* isomerization of phosphine complexes. Reductive elimination of Int_{3b} can readily occur at a barrier of 11.5 kcal mol⁻¹, and this barrier is rather low partially because of the steric assistance: the repulsion between the two *cis* phosphine ligands is partially released when the final product is formed. In addition, the ligands experience minimal reorganization during the reductive elimination. The overall reaction is slightly exergonic by 6.7 kcal mol⁻¹. It should be noted that although DFT studies seemingly suggest a positive ΔS^\ddagger with the dissociation of a phosphine ligand, the entropy change was overlooked. Solvent reorganization or polarization by a cationic metal center may contribute to a

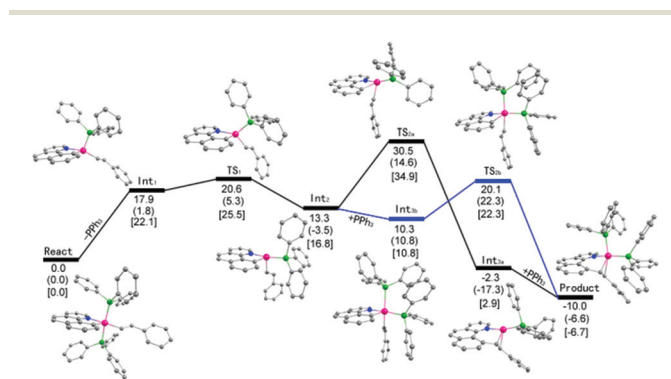
slightly negative ΔS^\ddagger . Clearly, path (b) is preferred. The calculated energy profile is in both qualitative and quantitative agreement with the experimental data in terms of the activation energy and the rate law of the phosphine. The calculated highest barrier of $\Delta G^\ddagger = 25.5$ kcal mol⁻¹ represents the barriers of the dissociation of the phosphine ligand. This theoretical value stays in line with the experimental value of $\Delta G^\ddagger = 23.6$ kcal mol⁻¹ derived from the rate constant of 8.6×10^{-3} min⁻¹ at 293 K (Table 2, entry 2). In addition to these two possible pathways, direct reductive elimination of the starting complex has been attempted, and indeed a significantly higher kinetic barrier was located.

While the fact that the C–C reductive coupling occurred at a higher rate in oxygen-containing solvents may not lead to any solid conclusion on the intermediacy of the kinetically important species (both four and five coordinate species remain possible), our DFT studies provided further evidence. Our solvent-dependent kinetics is at least consistent with the DFT studies. The starting *trans* phosphine complex is kinetically inert and cannot undergo direct C–C reductive coupling. In a more coordinating solvent, the dissociation of one of the phosphine ligands is facilitated because the resulting four coordinate intermediate Int1 is coordinatively unsaturated and can be better stabilized. This extra stabilization does not exist in a poorly coordinating solvent such as CH₂Cl₂.

Conclusions

A series of rare five-coordinate [Rh(C[∧]N)(PAR₃)₂(CH=CHR)]–PF₆ complexes have been isolated from the insertion of alkyne into stable Rh(III) hydrides. These five-coordinate complexes are kinetically labile at room temperature and undergo clean reductive coupling to afford stable Rh(I) alkene complexes [Rh(N[∧]C–CH=CHR)(PAR₃)₂]PF₆. Thus direct observation of C–C reductive coupling from five-coordinate *d*⁶ transition metals has been made, and mechanistic details of this process have been studied by a combination of experimental and theoretical approaches.

Activation parameters were obtained from temperature-dependent kinetic studies. The solvent effect and the electronic effects of the reactive and ancillary ligands have been established, where the electronic effects pointed to typical ground state electronic influences. Introduction of phosphine has an inhibitive effect on the rate of decay and the phosphine concentration-dependent studies suggest that dissociation of a phosphine is involved. Thus the intermediacy of a four-coordinate intermediate plays an important role. Weakly coordinating oxygen-containing solvents tend to favor the reductive elimination possibly by ligation and stabilization of a lower-coordinate intermediate. The phosphine concentration-dependent studies suggest reversible phosphine dissociation and a four-coordinate intermediate is involved. Two mechanistically distinct pathways have been suggested based on experimental studies.



Scheme 7 DFT studies of energy profiles of two possible pathways. (a) Values (ΔE) without any parentheses are total energy changes with correction of the zero-point energy. (b) Values (ΔG°) in parentheses are Gibbs free energy where translation, rotation, and vibration movements are taken into consideration to estimate the thermal entropy and free energy. (c) Values (ΔG^\ddagger) in square brackets are Gibbs free energy where only vibration movements are taken into consideration to estimate the thermal entropy and free energy.

DFT studies have been applied to distinguish between these two possible pathways. It turned out that although a four-coordinate intermediate is involved, it does not undergo direct C–C reductive elimination to give a three coordinate olefin complex intermediate. Instead, recoordination of the departed phosphine ligands yields an isomerized *cis* phosphine intermediate that is the active species toward C–C reductive elimination. The DFT studies revealed that phosphine dissociation is rate-limiting and the activation free energy is in good agreement with the experimental result. The five-coordinate Rh(III) and the coupled Rh(I) complexes obtained in our system offered direct experimental data for related catalytic C–H activation and C–C coupling reactions since C–C reductive elimination studies are particularly rare for cationic complexes. Insights gained in this work may provide useful information for the design of new catalysts for C–C coupling.

Acknowledgements

We thank the Dalian Institute of Chemical Physics, Chinese Academy of Sciences and School of Physical and Mathematical Sciences, Nanyang Technological University, for financial support. Financial support from the NSFC is also gratefully acknowledged (no. 21272231). We thank Dr Yongxin Li for crystallographic analyses.

Notes and references

- 1 S. Murai, F. Kakiuchi, S. Sekine, Y. Tanaka, A. Kamatani, M. Sonoda and N. Chatani, *Nature*, 1993, **366**, 529.
- 2 B. M. Trost, *Angew. Chem., Int. Ed.*, 1995, **34**, 259.
- 3 W. D. Jones, *Topics in Organometallic Chemistry*, ed. S. Murai, Springer-Verlag, New York, 1999, vol. 3, p. 9.
- 4 F. Kakiuchi and S. Murai, *Topics in Organometallic Chemistry*, ed. S. Murai, Springer-Verlag, New York, 1999, vol. 3, p. 47.
- 5 V. Ritleng, C. Sirlin and M. Preffer, *Chem. Rev.*, 2002, **102**, 1731.
- 6 K. Fagnou and M. Lautens, *Chem. Rev.*, 2003, **103**, 169.
- 7 F. Kakiuchi, *Top. Organomet. Chem.*, 2007, **24**, 1.
- 8 D. A. Colby, R. G. Bergman and J. A. Ellman, *Chem. Rev.*, 2010, **110**, 624.
- 9 X. Wang, L. Zhou and W. Lu, *Curr. Org. Chem.*, 2010, **14**, 289.
- 10 D. J. Schipper, M. Hutchinson and K. Fagnou, *J. Am. Chem. Soc.*, 2010, **132**, 6910.
- 11 D. A. Colby, A. S. Tsai, R. G. Bergman and J. A. Ellman, *Acc. Chem. Res.*, 2012, **45**, 814.
- 12 P. B. Arockiam, C. Bruneau and P. H. Dixneuf, *Chem. Rev.*, 2012, **112**, 5879.
- 13 (a) G. Y. Song, F. Wang and X. Li, *Chem. Soc. Rev.*, 2012, **41**, 3651; (b) T. Satoh and M. Miura, *Chem. – Eur. J.*, 2010, **16**, 11212; (c) F. W. Patureau, J. Wencel-Delord and F. Glorius, *Aldrichimica Acta*, 2012, **45**, 31; (d) N. Kuhl, N. Schroder and F. Glorius, *Adv. Synth. Catal.*, 2014, **356**, 1443; (e) G. Song and X. Li, *Acc. Chem. Res.*, 2015, **48**, 1007. For a report on rhodium-catalyzed C–H activation that generated olefinated arenes bearing a heteroarene directing group (related to the chelating ligand in products 3 in this work), see: (f) N. Schroder, T. Besset and F. Glorius, *Adv. Synth. Catal.*, 2012, **354**, 579.
- 14 K. Gao and N. Yoshikai, *Acc. Chem. Res.*, 2014, **47**, 1208.
- 15 (a) D. M. Crumpton and K. I. Goldberg, *J. Am. Chem. Soc.*, 2000, **122**, 962; (b) D. M. Crumpton-Bregel and K. I. Goldberg, *J. Am. Chem. Soc.*, 2003, **125**, 9442; (c) K. L. Arthur, Q. L. Wang, D. M. Bregel, N. A. Smythe, B. A. O'Neill, K. I. Goldberg and K. G. Moloy, *Organometallics*, 2005, **24**, 4624; (d) J. Procelewska, A. Zahl, G. Liehr, R. V. Eldik, N. A. Smythe, B. Scott Williams and K. I. Goldberg, *Inorg. Chem.*, 2005, **44**, 7732; (e) A. T. Luedtke and K. I. Goldberg, *Inorg. Chem.*, 2007, **46**, 8496.
- 16 T. Korenaga, K. Abe, A. Ko, R. Maenishi and T. Sakai, *Organometallics*, 2010, **29**, 4025.
- 17 M. P. Lanci, M. S. Remy, D. B. Lao, M. S. Sanford and J. M. Mayer, *Organometallics*, 2011, **30**, 3704.
- 18 (a) A. Ariafard and B. F. Yates, *J. Organomet. Chem.*, 2009, **694**, 2075; (b) A. Ariafard, Z. Ejehi, H. Sadrara, T. Mehrabi, S. Etaati, A. Moradzadeh, M. Moshtaghi, H. Nosrati, N. J. Brookes and B. F. Yates, *Organometallics*, 2011, **30**, 422.
- 19 (a) A. J. Canty, in *Comprehensive Organometallic Chemistry*, ed. R. J. Puddephatt, Pergamon, New York, 2nd edn, 1995, vol. 9, Chapter 5; (b) D. Kruis, M. A. Markies, A. J. Canty, J. Boersma and G. van Koten, *J. Organomet. Chem.*, 1997, **532**, 235; (c) A. J. Canty, J. L. Hoare, N. W. Davies and P. R. Traill, *Organometallics*, 1998, **17**, 2046; (d) A. J. Canty, J. L. Hoare, J. Patel, P. M. Feffer, B. W. Skelton and A. H. White, *Organometallics*, 1999, **18**, 2660; (e) A. Bayler, A. J. Canty, P. G. Edwards, B. W. Skelton and A. H. White, *J. Chem. Soc., Dalton Trans.*, 2000, 3325.
- 20 J. F. Hartwig, *Inorg. Chem.*, 2007, **46**, 1936.
- 21 B. L. Madison, S. B. Thyme, S. Keene and B. S. Williams, *J. Am. Chem. Soc.*, 2007, **129**, 9538.
- 22 (a) V. P. Ananikov, D. G. Musaev and K. Morokuma, *J. Am. Chem. Soc.*, 2002, **124**, 2839; (b) V. P. Ananikov, D. G. Musaev and K. Morokuma, *Organometallics*, 2005, **24**, 715; (c) V. P. Ananikov, D. G. Musaev and K. Morokuma, *Eur. J. Inorg. Chem.*, 2007, 5390; (d) V. P. Ananikov and I. P. Beletskaya, *Chem. – Asian J.*, 2011, **6**, 1423.
- 23 (a) R. A. Widenhoefer and S. L. Buchwald, *J. Am. Chem. Soc.*, 1998, **120**, 6504; (b) M. R. Biscoe, T. E. Barder and S. L. Buchwald, *Angew. Chem., Int. Ed.*, 2007, **46**, 7232.
- 24 (a) J. M. Racowski, A. R. Dick and M. S. Sanford, *J. Am. Chem. Soc.*, 2009, **131**, 10974; (b) N. D. Ball, J. B. Gary, Y. Ye and M. S. Sanford, *J. Am. Chem. Soc.*, 2011, **133**, 7577; (c) A. M. Wagner, A. J. Hickman and M. S. Sanford, *J. Am. Chem. Soc.*, 2013, **135**, 15710.
- 25 C. Hahn, M. Spiegler, E. Herdtweck and R. Taube, *Eur. J. Inorg. Chem.*, 1999, 435.

- 26 J. Navarro, E. Sola, M. Martín, I. T. Dobrinovitch, F. J. Lahoz and L. A. Oro, *Organometallics*, 2004, **23**, 1908.
- 27 (a) X. Li, C. D. Incarvito and R. H. Crabtree, *J. Am. Chem. Soc.*, 2003, **125**, 3698; (b) X. Li, L. N. Appelhans, J. W. Faller and R. H. Crabtree, *Organometallics*, 2004, **23**, 3378.
- 28 M. A. Esteruelas, F. J. Fernández-Alvarez, M. Oliván and E. Oñate, *J. Am. Chem. Soc.*, 2006, **128**, 4596.
- 29 S. H. Wiedemann, J. C. Lewis, J. A. Ellman and R. G. Bergman, *J. Am. Chem. Soc.*, 2006, **128**, 2452.
- 30 L. Benhamou, V. César, N. Lugan and G. Lavigne, *Organometallics*, 2007, **26**, 4673.
- 31 K. J. Hawkes, K. J. Cavell and B. F. Yates, *Organometallics*, 2008, **27**, 4758.
- 32 R. Ghosh, T. J. Emge, K. Krogh-Jespersen and A. S. Goldman, *J. Am. Chem. Soc.*, 2008, **130**, 11317.
- 33 H. Xu and W. H. Bernskoetter, *J. Am. Chem. Soc.*, 2011, **133**, 14956.
- 34 R. J. Pawley, M. A. Huertos, G. C. Lloyd-Jones, A. S. Weller and M. C. Willis, *Organometallics*, 2012, **31**, 5650.
- 35 (a) N. Wang, B. Li, H. Song, S. Xu and B. Wang, *Chem. – Eur. J.*, 2013, **19**, 358; (b) G. Zhang, L. Yang, Y. Wang, Y. Xie and H. Huang, *J. Am. Chem. Soc.*, 2013, **135**, 8850; (c) M. Brasse, J. Campora, J. A. Ellman and R. G. Bergman, *J. Am. Chem. Soc.*, 2013, **135**, 6427.
- 36 B. Rybtchinski and D. Milstein, in *Activation and Functionalization of C-H Bonds*, ACS Symposium Series, American Chemical Society, Washington, DC, 2004, vol. 885, pp. 70–85.
- 37 (a) M. P. Brown, R. J. Puddephatt and C. E. E. Upton, *J. Organomet. Chem.*, 1973, **49**, C61; (b) M. P. Brown, R. J. Puddephatt and C. E. E. Upton, *J. Chem. Soc., Dalton Trans.*, 1974, 2457.
- 38 G. S. Hill, G. P. A. Yap and R. J. Puddephatt, *Organometallics*, 1999, **18**, 1408 and references therein.
- 39 R. Cohen, M. E. Van der Boom, L. J. W. Shimon, H. Rozenberg and D. Milstein, *J. Am. Chem. Soc.*, 2000, **122**, 7723.
- 40 (a) U. Fekl, W. Kaminsky and K. I. Goldberg, *J. Am. Chem. Soc.*, 2001, **123**, 6423; (b) U. Fekl and K. I. Goldberg, *J. Am. Chem. Soc.*, 2002, **124**, 6804; (c) U. Fekl, W. Kaminsky and K. I. Goldberg, *J. Am. Chem. Soc.*, 2003, **125**, 15286; (d) S. M. Kloek and K. I. Goldberg, *J. Am. Chem. Soc.*, 2007, **129**, 3460; (e) A. T. Luedtke and K. I. Goldberg, *Inorg. Chem.*, 2007, **46**, 8496; (f) M. L. Scheuermann, A. T. Luedtke, S. K. Hanson, U. Fekl, W. Kaminsky and K. I. Goldberg, *Organometallics*, 2013, **32**, 4752.
- 41 (a) D. Karshtedt, J. L. McBee, A. T. Bell and T. D. Tilley, *Organometallics*, 2006, **25**, 1801; (b) P. Sangtrirutnugul, M. Stradiotto and T. D. Tilley, *Organometallics*, 2006, **25**, 1607; (c) P. Sangtrirutnugul and T. D. Tilley, *Organometallics*, 2008, **27**, 2223.
- 42 (a) S. B. Zhao, G. Wu and S. Wang, *Organometallics*, 2008, **27**, 1030; (b) S. B. Zhao, Q. Cui and S. Wang, *Organometallics*, 2010, **29**, 998.
- 43 R. Tan and D. Song, *Inorg. Chem.*, 2011, **50**, 10614.
- 44 (a) R. Ghosh, X. Zhang, P. Achord, T. J. Emge, K. Krogh-Jespersen and A. S. Goldman, *J. Am. Chem. Soc.*, 2007, **129**, 853; (b) R. Ghosh, T. J. Emge, K. Krogh-Jespersen and A. S. Goldman, *J. Am. Chem. Soc.*, 2008, **130**, 11317.
- 45 S. Gatard, R. Çelenligil-Çetin, C. Y. Guo, B. M. Foxman and O. V. Ozerov, *J. Am. Chem. Soc.*, 2006, **128**, 2808.
- 46 (a) S. S. Chen, G. Y. Song and X. Li, *Tetrahedron Lett.*, 2008, **49**, 6929; (b) S. S. Chen, Y. Li, J. Zhao and X. Li, *Inorg. Chem.*, 2009, **48**, 1198.